Econ. Environ. Geol.
Vol. 31, No. 3, p. 235-247, 1998.

3-D Crustal Velocity Tomography in the Central Korean Peninsula

So Gu Kim* and Qinghe Li**

ABSTRACT : A new technique of simultaneous inversion for 3-D seismic velocity structure by using direct, reflected, and refracted waves is applied to the center of the Korean Peninsula including Pyongnam Basin, Kyonggi Massif, Okchon Fold Zone, Taebaeksan Fold Zone, Ryongnam Massif and Kyongsang Basin. Pg, Sg, PmP, SmS, Pn, and Sn arrival times of 32 events with 404 seismic rays are inverted for locations and crustal structure. 5 (1° along the latitude)×6 (0.5° along the longitude)×8 block (4 km each layer) model was inverted. 3-D seismic crustal velocity tomography including eight sections from the surface to the Moho, eight profiles along latitude and longitude and the Moho depth distribution was determined. The results are as follows: (1) the average velocity and thickness of sediment are 5.15 km/sec and 3~4 km, and the velocity of basement is 6.12 km/sec. (2) the velocities fluctuate strongly in the upper crust, and the velocity distribution of the lower crust under Conrad appears basically horizontal. (3) the average depth of Moho is 29.8 km and velocity is 7.97 km/sec. (4) from the sedimentary depth and velocity, basement thickness and velocity, form of the upper crust, the Moho depth and form of the remarkable crustal velocity differences among Pyongnam Basin, Kyonggi Massif, Okchon Zone, Ryongnam Massif and Kyongsang Basin can be found. (5) The different crustal features of ocean and continent crust are obvious. (6) Some deep index of the Chugaryong Rift Zone can be located from the cross section profiles. (7) We note that there are big anisotropy bodies near north of Seoul and Hongsung in the upper crust, implying that they may be related to the Chugaryong Rift Zone and deep fault systems.

INTRODUCTION

The tomographic inversion of local seismic travel time data has been become a very efficient technique to study the earth's 3-D crustal structure with ever-increasing availability of more powerful computers and higher quality of seismic data. Many scientists have their contribution for the seismic inversion methods (Aki, Lee, 1976; Backus, Gilbert, 1967; Benz, Smith, 1984; Crosson, 1976; Hawley *et al.*, 1981; Koch 1985a, b, 1993; Lees, Crosson, 1989; Liu, 1984; Sambridge, 1990; Tarantola, 1987, 1992; Thomson, Gubbins, 1982; Thurber, 1983, 1985; Walck, Clayton, 1987).

The major problem of seismic tomography inversion is the multi-solution. The coupling between hypocentres and seismic velocities causes the relative results of velocity and hypocentre. One procedure is decoupling of hypocentres from the structure which reduce the dimensions of the matrix of the Frechet derivative significantly, or the use of subspace method. The use of linear equations to non-linear inversion makes bias distortion of the result from practice. However, in case the initial model is well chosen and is sufficiently close to the true minimum of the objective function, a linear or at least a quasi-linear treatment appears to be vindicated. The ill-posed of the seismic inversion which is induced by the trade-off between hypocentres and seismic velocities is most complex. Whereas the concept of regularization is fairly well understood for linear inversion, one has to use a general theory for the non-linear inversion (Koch, 1993).

The increasing of independent parameters to attend inversion is the key for physical meaning. As we know, it is not increasing the amount of data (of course, the co-linear data are needed), but if the independent data which possess common physical base as constrained condition participates in inversion, these data may help to solve the puzzles of pure mathematical algorithm.

In this paper, we introduce the seismic inversion basic principle, constrained inversion methods, including P- and S- wave simultaneous inversion, combining the DSS and earthquake data, optimal regularization and error estimation. Pg, Sg, PmP, SmS, Pn, and Sn are common phases understood by most seismologists. The relative seismic phases have similar seismic ray paths, so they can mirror of the same interface. We can perform the inversion me-

* The Seismological Institute, Hanyang University, Ahnsan, Kyonggido, South Korea, 427-791
** Lanzhou seismological Institute, SSB Lanzhou, China 73000

thod by using them as constrained condition to reduce multi-solution of results. Because the rays of Pg, PmP, and Pn propagate through different parts of the crust, combining them can get the information from the top to the bottom of the crust. According to the above methods, the computer program "3DZL" was performed.

The Korean Peninsula is located near the boundary of the Pacific plate and the Eurasian plate. In the view of the plate motion, this peninsula is a transition zone of two plates. The deep structure can reflect the induction and deduction of plate motion. But up to now, there is blank for 3-D seismic velocity distribution. The central part of the Korean Peninsula is a tectonic complex region. The Pyongnam Basin, Imjingang Zone, Taebaeksan Zone, Okchon Zone, Kyonggi Massif, Ryongnam Massif, Kyongsang Basin, and the Pohang Basin line the NE direction. We give the 3-D seismic inversion tomographic results including eight sections from the surface to the Moho, thirteen (but only eight presented here) profiles along latitude and longitude respectively and the Moho depth distribution. According to these images, we analyzed the structural characteristics of sedimentary, basement, the upper crust, Conrad, the lower crust and the Moho. The major difference of deep structure for different geological province was investigated.

METHODOLOGY

Basic Principle

The general expression for the seismic traveltime T_{ij} between *ith* (i=2, 3,...m_e) event and *jth* (j=1,2,...n_s) station is:

$$T_{ij} = \int_{L_{ij}} u(\mathbf{r}) ds \tag{1}$$

where $\mathbf{r}$ is position vector, $u(\mathbf{r})=1/v(\mathbf{r})$ is wave slowness, $v(\mathbf{r})$ is velocity vector, L_{ij} is ray path between hypocentre and station, and ds is ray element.

The traveltime T is a non-linear function of velocity v. Using Fermat's principle, the first correction of traveltime is induced by the perturbation of wave slowness as well as the source unknown. So the perturbation equation can be written as (Liu, 1984)

$$\delta T_{ij} = \int_{L_{ij}} \delta u ds + \delta \mathbf{X}_{iq} \cdot \nabla_{x_i} T_{ij} \tag{2}$$

where x_{iq} (q=1, 2, 3, 4) are latitude, longitude, depth and original time of *ith* source.

For m_e events and n_s parameters of wave slowness

$$\mathbf{t} = cy \quad c = (A, B) \quad \mathbf{y} = (\delta v^T, \delta x^T)^T \tag{3}$$

where $\mathbf{t}$ is traveltime vector, c is coefficient matrix, and $\mathbf{y}$ is a solve vector including source parameter δx and model parameters δv.

$$\begin{aligned} &\mathbf{t} = (\mathbf{t}_1, \mathbf{t}_2, ... \mathbf{t}_{m_e})^T \\ &A = (A^1, A^2, ... A^{m_e})^T \\ &B = diag(B^1, B^2, ... B^{m_e}) \end{aligned} \tag{4}$$

$$A_{ij} = \int_{L_{ij}} \frac{\partial u}{\partial v_q} ds \tag{5}$$

$$B_{ij} = \frac{\partial T_{ij}}{\partial x_{ik}}$$

$$\begin{aligned} &l = n_e(i-1) = j \\ &q = 4(i-1) + k \end{aligned} \tag{6}$$

where $m=m_e \times n_s$, A *is* $m \times n$ matrix, B is $m \times 4m_e$ matrix, $\mathbf{t}$ is the residual time vector of m dimensions, if $t_{ij}^{(O)}$ tis observational arrival time, O_i is "guess" original time, then:

$$\begin{aligned} &t_i = t_{ij}^{(O)} - O_i - T_{ij}, \\ &l = n_s(i-1) + j \end{aligned} \tag{7}$$

$$\begin{aligned} &\delta \mathbf{x} = (\delta \mathbf{x}_1, \delta \mathbf{x}_2, \cdots \delta \mathbf{x}_{m_e})^T \\ &\delta \mathbf{v} = (\delta \mathbf{x}_1, \delta \mathbf{v}_2, \cdots \delta \mathbf{v}_{m_e})^T \end{aligned} \tag{8}$$

Under non-constrained condition, the solution vector of equation (3) can be indicated as minimum norm

$$||\mathbf{t} - c\mathbf{y}||_2^2 = \min \tag{9}$$

The formula (9) is equivalent to minimum norm solution δv.

If the orthogonal projection operator of image space $\Gamma(B)$ in which ϖ^n project to B, B^+ is general Moore-Penrose inverse matrix of B, was written as $P_B=BB^+$, then (9) can be rewritten as

$$\begin{aligned} &||\mathbf{t} - c\mathbf{y}||_2^2 = ||\mathrm{P_B}(\mathbf{t} - c\mathbf{y})||_2^2 + \\ &||(I - P_B)(\mathbf{t} - c\,\mathbf{y})||_2^2 = \min \end{aligned} \tag{10}$$

where I is unit matrix, insert (3) to (10), then

$$\begin{aligned} &||\mathbf{t} - c\mathbf{y}||_2^2 = ||P_B(\mathbf{t} - \mathrm{A}\delta v) - \mathrm{B}\delta \mathbf{x}||_2^2 + \\ &||(I - P_B)\mathbf{t} - (I - P_B)A\,\delta \mathbf{v}||_2^2 = \min \end{aligned} \tag{11}$$

(11) is equivalent to minimum norm solution $\delta\hat{v}$ and $\delta\hat{x}$ respectively:

$$||(I - P_B)\mathbf{t} - (I - P_B)A\,\delta\hat{v}||_2^2 = \min \tag{11a}$$

$$||P_B(\mathbf{t} - A\,\delta\hat{\mathbf{v}}) - B\,\delta\hat{\mathbf{x}}||_2^2 = \min \tag{11b}$$

After some calculating, we can get the model estimation of and respectively.

Constrained Inversion

P and S Simultaneous Inversion

We know that an earthquake source can emit P and S waves for the spherical surface. Since P and S waves can reflect the same interface, we can use the simultaneous inversion as constrained conditions to reduce multi-solution of the inversion. Because Pg and Pn phases can be distinguished easily as the first arrivals in various distances, the amplitude of PmP is stronger in suitable distance, so Pg, Pn, PmP, and corresponding Sg, Sn, and SmS are common phases understood by most seismologists. The rays of Pg, PmP, and Pn propagate through different paths of the crust, so the combining of them can get the information from the top to the bottom of the crust, and especially the seismic rays from PmP and Pn also can thread in up-going to the upper crust, so the information density in the upper crust is estimated.

In this study we use Pg, Sg, PmP, SmS, Pn, and Sn to inverse the whole crust for increasing the constrained condition for inversion.

Combining DSS and Earthquake Data to the Simultaneous Inversion.

Since DSS (deep seismic sounding) data have more accurate location, original time and dense stations on line, so the quality of result of DSS is higher than earthquakes.

Assume there are m_1 explosions and m_2 earthquakes, then equation (11) can be rewritten as (Li *et al.*, 1994)

$$||P_1 - P_2||_2^2 = \min \tag{12}$$

$$P_1 = \begin{bmatrix} \mathbf{t}_{m_1} \\ (I - P_B)\mathbf{t}_{m_2} \end{bmatrix} \quad P_2 = \begin{bmatrix} A_{m_1} \\ (I - P_B)A_{m_2} \end{bmatrix} \tag{13}$$

If we set velocity constrain for 2-D velocity structure from DSS, then (12), (13) can be rewritten as

$$||P_3 - P_4||_2^2 = \min \tag{14}$$

$$P_3 = \begin{bmatrix} \mathbf{v}_{m_1} \\ (I - P_B)\mathbf{t}_{m_2} \end{bmatrix} \quad P_4 = \begin{bmatrix} A_{m_1} \\ (I - P_B)A_{m_2} \end{bmatrix} \tag{15}$$

where v_{m_i} denotes velocity known.

If there are several DSS lines across on the same area, we can construct them as a fixed model to use above formulae (12-15).

Optimal Regularization

We select the Levenberg-Marquardt method to get the optimal regularization. It is demonstrated that the LM method, in spite of its computational inexpediences, has various properties that make it best suited for the solution of both the general non-linear inverse problem and its linearized subproblems (Koch, 1993).

Database

We constructed database to get the results of profiles to analyze the velocity distribution as depth directly.

Error Estimation

Following equations are used for estimating resolution and error.

a) The resolution of the model is computed from the resolution matrix

$$\mathbf{R} = (\mathbf{B}^T\mathbf{B} + k\mathbf{I})^{-1}\mathbf{B}^T\mathbf{B} \tag{16}$$

b) The covariance of solution is

$$\mathrm{cov}(\delta v) = (\mathbf{B}^T\mathbf{B} + k\mathbf{I})^{-1}\mathbf{R}\sigma^2 \tag{17}$$

In (16) and (17), **R** is resolution matrix, **B** is Jacobian matrix and $\mathbf{B}=\nabla\mathrm{T}$, $\mathbf{B}^{\mathrm{T}}$ is a transposed matrix of **B**, **I** is unit matrix, δv is model vector, σ^2 is the variance of the data which is either estimated *a priori* or is evaluated from the *a posteriori* residual sum squared.

GEOLOGICAL BACKGROUND OF RESEARCH AREA

The Korean peninsula constitutes in general, the eastern part of the Sino-Korean Paraplatform. In our research area, the Pyongnam Basin, Kyonggi Massif, Okchon Folded Zone, Ryongnam Massif and Kyongsang Basin are major geological provinces. The Pyongnam Basin is located in the south of the Nangnim Massif and to the north of the Kyonggi Massif, and extends from the Yellow Sea in the west, to the East Sea in the east. The basin area was separated into three small subsidiary basins where the Pyongnan supergroup of Late Carboniferous to Early Triasic age was deposited. The Pyongnam Basin is the type locality in Korea where the paleozoic strata were classified and designated. The Pyongnam Basin is characterized generally by a

complex synclinorium where east-west trending folds and overthrusts are well developed. The Kyonggi Massif defined here includes the Yonbaek Massif and the Ongin Basin, both of which were previously denominated as independent provinces. The Kyonggi Massif is located in the central part of the Korean Peninsula and borders the Pyongnam Basin to the north, and on the Okchon Folded Zone. The massif is believed to be a part of the Sino-Korean Para-platform as the Nangnim Massif is. The Okchon Folded Zone is situated between the Kyonggi Massif to the north and the Ryongnam Massif to the south, and extends from southwest to northeast diagonally across the Korean Peninsula with an average breadth of 70 km. The Ryongnam Massif is situated in the southern part of the Korean Peninsula bounded by a fault with the Okchon Folded Belt on the northwest and the Kyongsang Basin on the southeast, and divided into the Taebaeksan Subzone in the northeastern part and the Chirisan Subzone in the

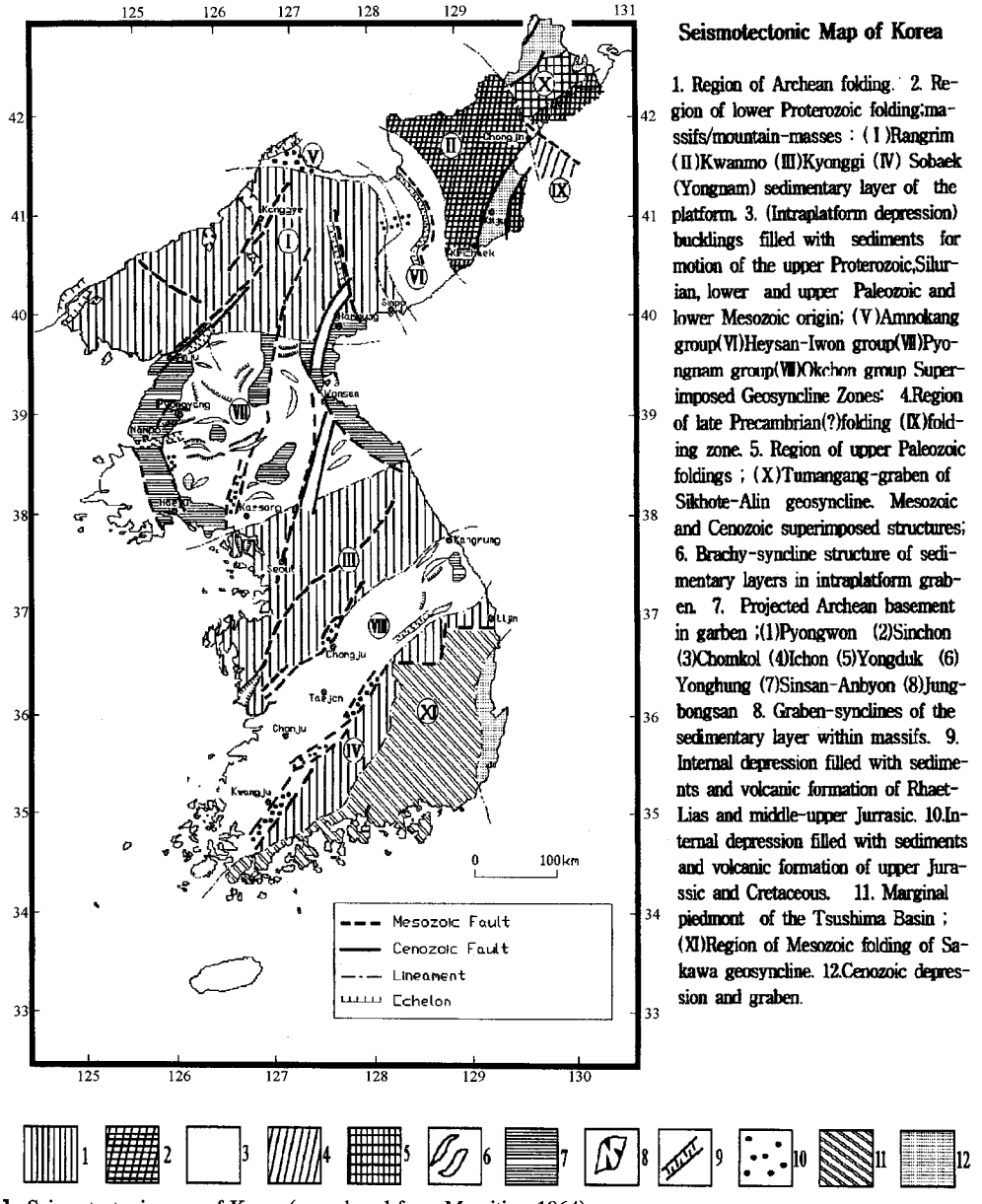

Seismotectonic Map of Korea

1. Region of Archean folding. 2. Region of lower Proterozoic folding;massifs/mountain-masses : (Ⅰ)Rangrim (Ⅱ)Kwanmo (Ⅲ)Kyonggi (Ⅳ) Sobaek (Yongnam) sedimentary layer of the platform. 3. (Intraplatform depression) bucklings filled with sediments for motion of the upper Proterozoic,Silurian, lower and upper Paleozoic and lower Mesozoic origin; (Ⅴ)Amnokang group(Ⅵ)Heysan-Iwon group(Ⅶ)Pyongnam group(Ⅷ)Okchon group Superimposed Geosyncline Zones: 4.Region of late Precambrian(?)folding (Ⅸ)folding zone. 5. Region of upper Paleozoic foldings ; (Ⅹ)Tumangang-graben of Sikhote-Alin geosyncline. Mesozoic and Cenozoic superimposed structures; 6. Brachy-syncline structure of sedimentary layers in intraplatform graben. 7. Projected Archean basement in garben ;(1)Pyongwon (2)Sinchon (3)Chomkol (4)Ichon (5)Yongduk (6) Yonghung (7)Sinsan-Anbyon (8)Jungbongsan 8. Graben-synclines of the sedimentary layer within massifs. 9. Internal depression filled with sediments and volcanic formation of Rhaet-Lias and middle-upper Jurrasic. 10.Internal depression filled with sediments and volcanic formation of upper Jurassic and Cretaceous. 11. Marginal piedmont of the Tsushima Basin ; (Ⅺ)Region of Mesozoic folding of Sakawa geosyncline. 12.Cenozoic depression and graben.

Fig. 1. Seismotectonic map of Korea (reproduced from Masaitisa, 1964).

southwestern part by a wedge of Kyongsang Supergroup projecting westward into the middle part of the massif area. The Fig. 1 shows the seismotectonic map of Korea (Kim, Gao, 1995).

DATA PROCESSING

Data

There are 23 seismic stations including analog and digital recordings around research area, and Table 1 illustrates the station parameters. The data used in research area are local arrival times of 32 earthquakes occurring between 1982 and 1997. The local magnitudes (M_L) of the earthquakes range between $1.6<M_L<3.3$. Depending on their sizes, events have been recorded at 3~10 stations. The epicentral parameters were located by using HYPO71 by KMA and/or a single station of three components (Kim, Gao, 1997).

We analyze three seismic phases to inverse velocity structure and relocation.

a) Pg: The epicentral range of 20~120 km as first arrival pickings, they are direct waves, and they almost emitted upgoing from the source to stations. Because these phases are tip and clear, so the accuracy of them is higher, and can reach 0.1~0.2 sec.

b) PmP: The reflection waves from Moho, the epicentral range of 90~250 km to use, including overcritical distance. This phase has stronger amplitude even though it is a later arrival phase after some wavelet. The accuracy of picking up can reach about 0.2 sec.

c) Pn: The refraction wave along the Moho. From 160 km it can emerge as the first onset but amplitude is small. They are clearer and tip with increasing epicentral distance and the duration time between Pn and PmP are longer. However, because the energy from Pn is not stronger, the onset is not clear on some distance and the accuracy is not higher. We think the accuracy can reach about 0.2 sec.

d) S-wave including Sg, SmS, and Sn correspon-

Table 1. Station parameters.

Organization	Station	Latitude			Longitude			Elevation
		D	M	S	D	M	S	(Km)
KMA (analog)	Seoul	37	34	01	126	58	01	0.200
Whole Country	Kangneung	34	45	00	128	54	00	0.200
	Seosan	37	46	01	126	28	01	0.300
	Choopung	36	13	01	128	00	01	0.200
	Chunchon	36	54	00	127	43	59	0.200
	Daejon	37	18	00	127	24	00	0.200
	Ulchin	36	58	59	129	25	01	0.300
IRIS (digital) Inchon	Inchon	37	28	59	126	37	59	0.200
KIGAM (digital)	CHS	36	10	48	129	05	24	0.200
South and partly middle	DK	35	56	24	129	06	36	0.200
	JPCH	37	57	42	127	07	53	0.200
SIHY(digital)	Sy1111	37	34	31	128	16	33	0.768
Central Korean Peninsula	Sy1221	37	29	34	128	00	31	0.181
	Sy2113	37	30	01	127	38	01	0.220
	Sy2221	37	30	04	128	04	21	0.207
	Sy2331	37	32	08	127	50	09	0.465
	Sy1331	37	34	45	128	32	10	0.610
KSRS (digital) Wonju	Wonju	37	29	14	127	55	24	0.200
SIHY (digital)	Tem8	37	31	06	127	53	31	0.200
Central Korean Peninsula	Tem11	37	29	20	127	57	10	0.200
	Tem16	37	27	15	127	51	50	0.200
	Tem13	37	26	38	127	56	05	0.200

N.B. KMA (Korea Meteorological Administration), IRIS (Incorporated Research Institutions for Seismology), KSRS (Korea Seismological Research Stations), SIHY (Seismological Institute of Hanyang University), KIGAM (Korea Institute of Geology, mining, and Materials)

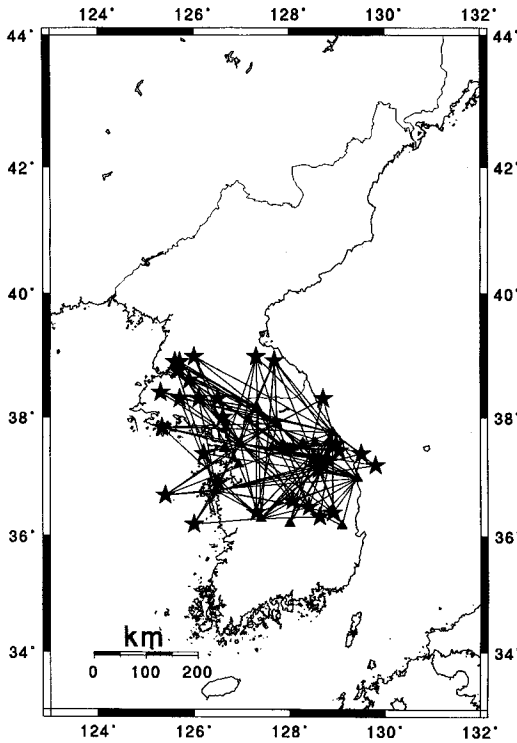

Fig. 2. Configuration for seismic rays between epicenters and stations. Stars and triangles indicate events and stations, respectively.

ding to Pg, PmP and Pn. They are later phases, so determining the arrival is difficult and the error will be larger. We think the accuracy will be about 0.2~0.3 sec.

The hypocentre determination is subject to certain quality criteria. Thus events are eliminated from the inversion if they occur outside the area of the model and the quality of the hypocentre location attributed by HYPO71 is not good for a certain threshold with less than three stations recorded. These criteria reduce the original events. Finally we select the data to inverse 32 events with 78 of Pg and Sg, 89 of PmP and SmS, and 35 of Pn and Sn in the research area. Fig. 2 illustrates stations, events and seismic rays in our research.

Configuration of Initial Models

We select a plane layer block model with discrete velocity parameters. For this model, each horizontal layer is divided into blocks of equal size. A constant velocity is defined with each block. Within each layer and among different layers the interpolating function was used. This makes the model applicable to 3-D ray tracing techniques. According to the data and geometry of research area, we determine the inversion model as follows:

Scope: 36°~39°N, 125°~130°E

Block: 5×6

Layer: 8 layers with 4 km each layer.

According to former research results (Kim, Kim, 1983; Kim, Jung, 1985; Kim, Lee, 1994), we try to calculate several models to test the stability of various models. After comparing them we determine the initial model as shown on Table 2.

Inversion Processing

We have an experiment to test the suitable model. The test results demonstrate that for various models, the Moho form, and the velocity distribution are basically similar. It means that the inversion method is independent of the initial model, and the result is stable. Of course, the model result is close to the actual practical situation.

The optimal solutions will then be retrieved using the various optimal regularization techniques of long objective and subjective evaluations of these models and of some personal judgement based on the practical experience of the author. The trade-off characteristics for regularization and resolution have to be carried out.

In addition, optimal solutions are also eventually based on the minimization criteria for the non-linear objective function, or the total residual sum. The RMS value of the traveltime residuals obtained for most of the seismic events lie in the range 0.1~0.2 sec. The standard deviations for the epicentral coordinates are 2 km, for the depth is 5 km. In our computer program, we have a termination criterion for the iteration. The final results are comfortable for the above conditions.

We produced eight isovelocity tomography sections corresponding to the stratified model. Moho distribution was also determined. According to mode, we construct ten seismic profiles along latitude and

Table 2 Initial model.

Layer	1	2	3	4	5	6	7	8
Depth (km)	0~4	4~8	8~12	12~16	16~20	20~24	24~28	28~32
Velocity (km/sec)	5.10	6.20	6.35	6.50	6.70	6.96	7.45	8.05

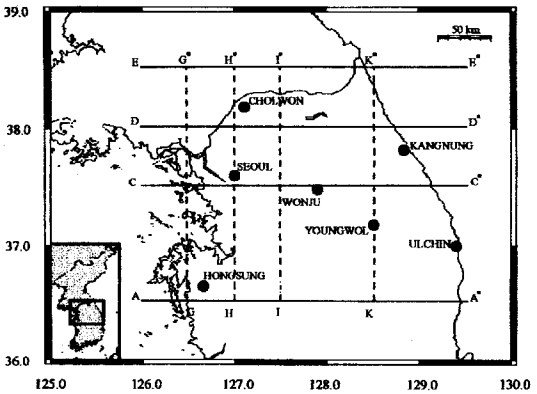

Fig. 3. Map shows the study area and the seismic profile lines in the Central Korean Peninsula.

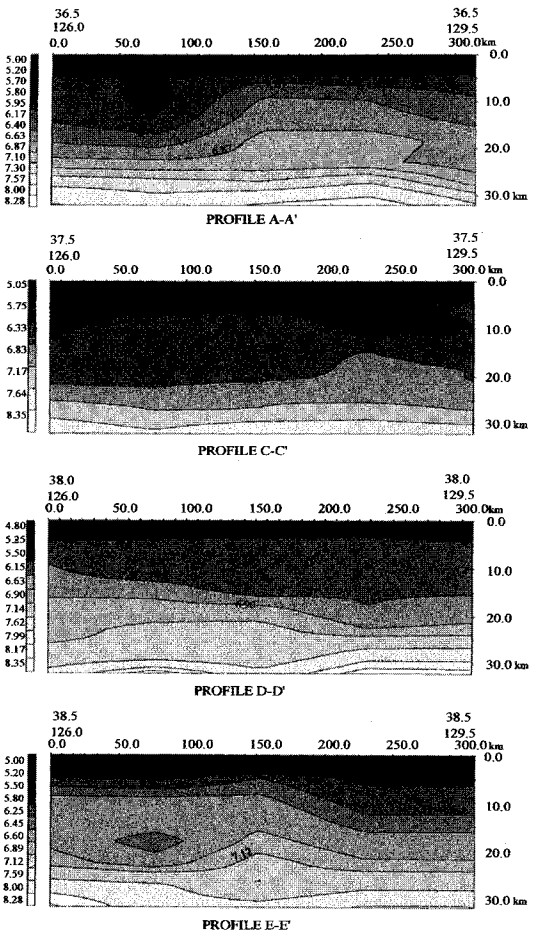

Fig. 4a. The cross section of the seismic profiles along the vertical planes; A-A', C-C', D-D', and E-E'.

longitude. These images show as figures to figures. The confidences of results in four corners are less

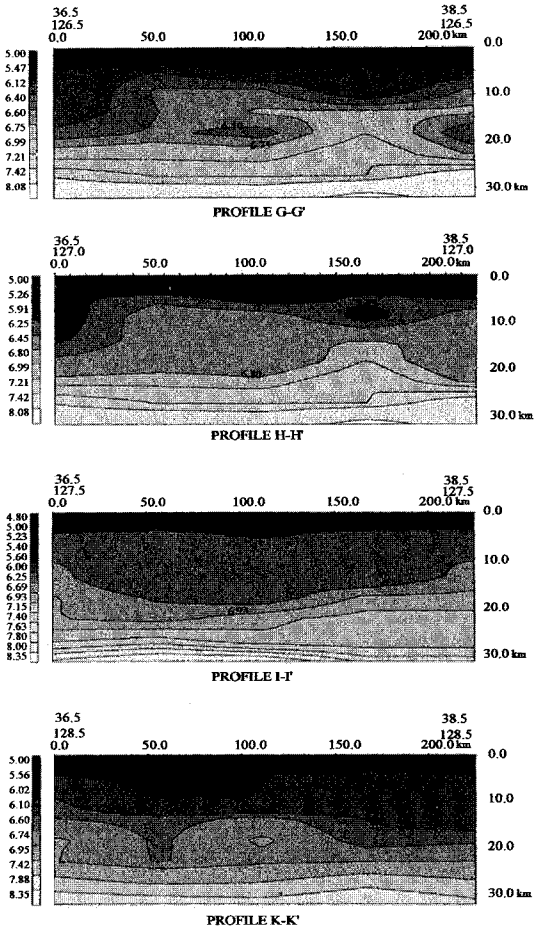

Fig. 4b. The same as Fig. 4a for G-G', H-H', and K-K'.

because there are few seismic rays through those areas. Fig. 3 shows the study area and the seismic profile lines in the Central Korean Peninsula.

The inversion scope and profiles are shown in Fig. 4 and 5 show the tomographic sections from surface to Moho. Fig. 6 shows the Moho distribution.

Since there are not any data in the block with 38°~39°N, 129°~130°E and in addition, in 125°~125.5°E, 129.5°~130°E, the data are rare, so the confidence of result in above area is less.

MAJOR RESULTS

Sedimentary Layer and Basement

Combining the profiles (see Fig. 3) and cross sections (see Fig. 4 and 5), we can get the basement and sedimentary layer information. The average velocity in sedimentary is about 5.15 km/sec in general, but in

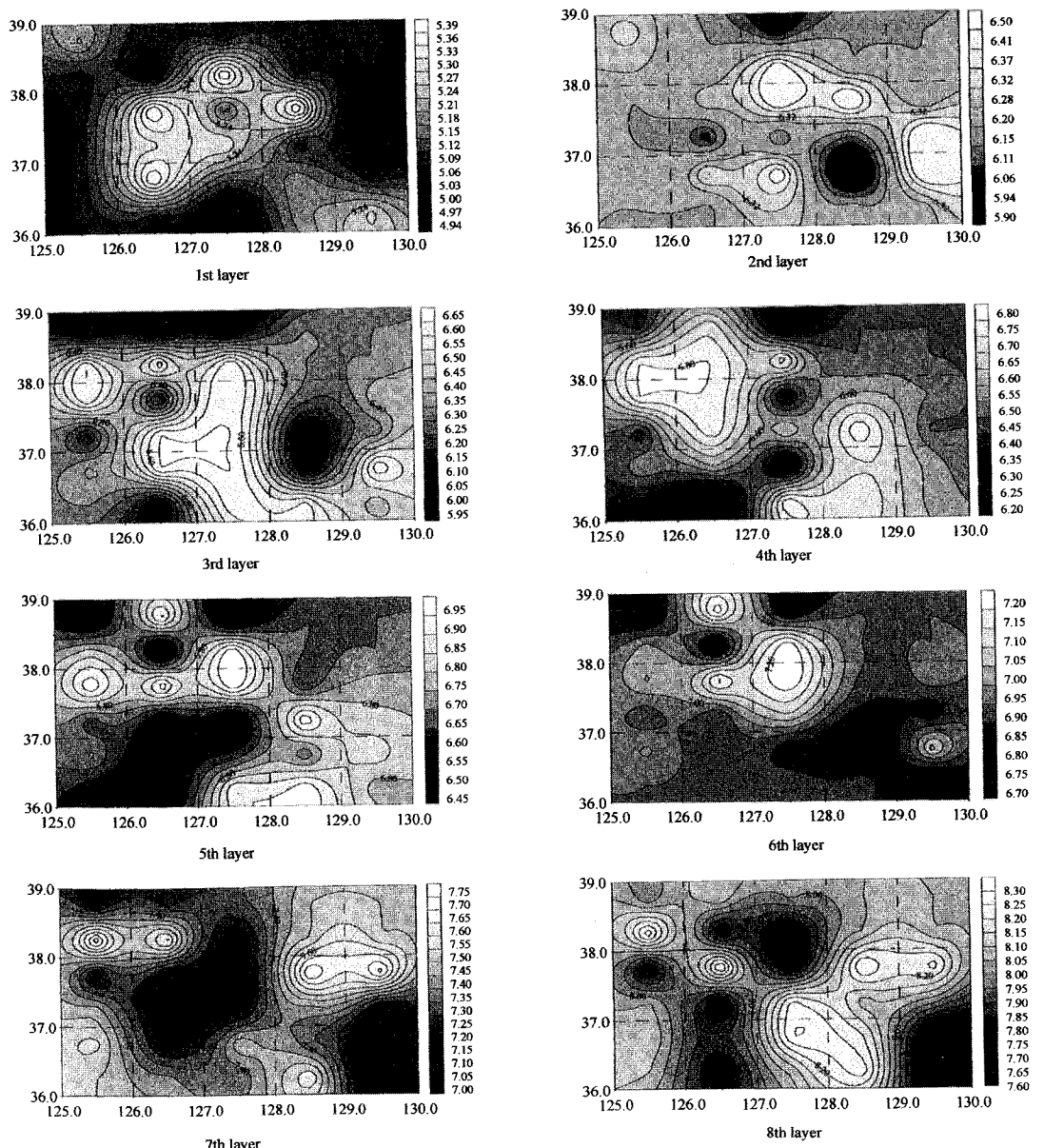

Fig. 5. The isovelocity map along the horizontal plane. Earth block thickness is 4 km including the first through the eighth layer.

some regions it can reach 5.5 km/sec. The depositing thickness of sediments is about 3.31 km in general, but for various regions they are not the same. The deepest is 5.5 km, in some areas, and the shallowest one is about 2.5 km. The sedimentary layer has 4-5 velocity strata; they are 5.16, 5.45, 5.72, and 5.95 km/sec respectively. Due to the limitation of the figure resolution scale, the surface layer with lower velocity has not been displayed.

The area with deeper sediments is around Seoul, Paektok-san, Chechon, Wonju, Chunchon, and Soyang Lake. The other area with deeper sediments is in the west and northwest of Kaesung, i.e. Namp'o plain. The area with shallower sediments is around Taejon, Chongju, Andong and Yongju. From Fig. 5, we can find the line with NE-SW direction dividing the velocity into higher and lower two parts is basically along the boundary line between Kyonggi

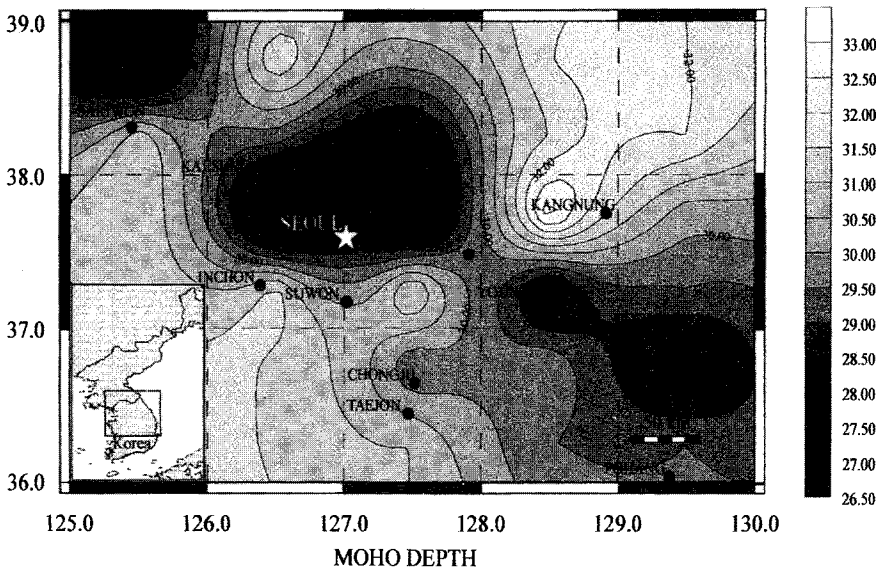

Fig. 6. Moho distribution on the Central part of the Korean Peninsula. The crustal thickness of Seoul, Wonju, Youngwol is 28.9, 30.3, and 28.9 km respectively. South and east of Seoul have a thicker crust.

Massif and Okchon Zone. That is, in the Kyonggi Massif, the velocities are higher and in the Okchon Zone are lower. A lower velocity area embedded in higher velocity area is in the northeast of Seoul, around Chunchon, and other lower velocity area is around 38.5°~39°N, 126°E, that is, near Nung-ni, Suan and Sangwon. Around the Daejon, there is a lower velocity area with 5.0~5.09 km/sec. The average basement velocity is 6.15 km/sec, the highest is 6.23 km/sec and the lowest is 6.01 km/sec.

Conrad

In the result of tomography research, we can find that there is a velocity discontinuous layer divided into the upper and lower. The characteristics of isovelocity contour in the two parts are remarkably different. This interface is Conrad discontinuity. In the upper crust, the velocity distribution forms fluctuate obviously, some higher (lower) velocity layer (body) embedded in normal layer. But in the lower crust, the horizontal velocity layer can be normally displayed.

The average velocity on the Conrad layer is about 7.10 km/sec, the highest is 7.17 km/sec, and the lowest is 6.97 km/sec. The average depth of the Conrad is 21.3 km with the deepest of 25.1 km and the shallowest of 16.6 km. We can find that the variation form of Conrad can reflect the major difference among different tectonic geological province, continent and ocean.

Moho

Fig. 6 is the Moho depth distribution. The average depth and velocity of Moho in research area is 29.8 km (the results in rare data are not calculated) and 7.97 km/sec with 8.04 km/sec (highest) and 7.85 km/sec (lowest) respectively.

The form represents deeper in NE and SW, shallower in NW and SE. The areas of shallower Moho are:

a) South of 37.5°N, east of 128°E, other three angle area with 36°~37°N, 127°~128°E , the tip point is 36.6°N, 126.7°E, the depth of Moho are 27.8~30.8 km, mostly 28.9~29.8 km. The Daejon, Chungju, Uljin, and Pohang are in this area. This area belongs to Kyongsang Basin, Okchon Fold Zone and Taebaeksan Zone.

b) The area with 37.4°~39°N, 125.5°~128.1°E (around Seoul, Inchon, Haeju, Kaesung and its northwest), the area with most shallow depth is in 37.7°~38.1°N, 126.1°~127.6°E with 26.4 km, it is located on the north of Seoul, including Kaesung and Chunchon.

c) The area with 38.5°~39°N, 125°~126°E (around Namp'o, Pyongyang), the depths are 26.4~30.1 km.

The deeper Moho areas are in 37.7°~38.2°N and 128.6°~129.1°E (around the Odaesan National Park of the northwest of Kangnung). However, the Moho depth of ocean area in above scope are shallower, but there are not seismic ray pass and the initial

Moho of 32 km induce a smoothing deeper depth.

Major Characteristics of the Crust

The crust of research area can be divided into upper and lower parts with the interface Conrad. From surface to 20~21 km is the upper crust. The upper crust has four velocity layers except sedimentary layer.

The average velocity of 1st layer under sediment is 5.24 km/sec. This layer is basically horizontal and the thickness is 1.5~2.5 km in general, and the thickest one is 5 km and the shallowest one is 1 km. The average velocity of 2nd layer is 6.40 km/sec and the highest is 6.49 km/sec, the lowest is 6.30 km/sec. The thickness of isovelocity changes from 1 km to 10 km, appearing stronger inhomogeneity. The average velocity of 3rd layer is 6.63 km/sec and the highest is 6.69 km/sec, the lowest is 6.52 km/sec. The thickness varies from 2 km to 15 km. The average velocity of 4th layer is 6.86 km/sec, the highest is 6.95 km/sec and the lowest is 6.73 km/sec. The thickness varies from 10 km to 15 km and the inhomogeneity can be found. A remarkable feature of the lower crust appears basically the horizontal. The depth from 21.3 km to Moho (29.8 km) is the scope of the lower crust. There are three velocity layers in the lower crust. The 5th layer has average velocity of 7.10 km/sec and 4.3 km of thickness, it is the Conrad layer. The 6th layer has average velocity of 7.36 km/sec and 2.7 km of thickness. The 7th layer has average velocity of 7.54 km/sec and 2.2 km of thickness.

The stronger inhomogeneous upper crustal velocities and horizontal stratified lower crust may indicate that the tectonic movement happened mainly in the upper crust. In contrast to some area of the inter-plate where the Moho and the lower crust have stronger inhomogeneity, the lower crust form may reflect that the tectonics and movement manner, evolution and geodynamics in this area are not similar to the plate boundaries.

From the profile A-A' (36.5°N, 126°E~36.5°N, 129.5°E), we find some important information a) There is a lower velocity body with 5.93 km/sec embedded in 6.40 km/sec layer, its buried depth is 5-10 km, the location on the surface between the Hongsung and Kongju, a big earthquake of M=7.0, occurred in July 20, 1594, as well as the recent earthquake, Hongsung earthquake of October 10, 1978 (M=5.0). b) The isovelocity of 6.4 km/sec layer has deeper thickness in the west of 125 km from the west starting point of the profile, but after 125 km, the 6.63 km/sec layer uplift into 6.40 km/sec. The

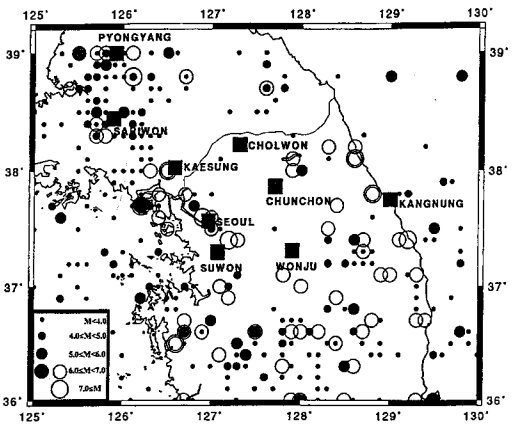

Fig. 7. Seismicity in the Central Korean Peninsula. Closed and open circles indicate instrumental (1905~1997) and historical (A.D. 2~1904) earthquakes, respectively.

125 km is a boundary of Kyonggi Massif and Okchon Zone. At 200 km from the west point of the profile the 6.87 km/sec layer uplift, this position is a boundary between Ryongnam Massif and Kyongsang Basin.

In the profile C-C' (37.5°N, 126°E~37.5°N, 129.5°E), the 6.46 km/sec layer uplift in the 75 km away (near Seoul) from the west point of the profile, correspondingly, the Moho is lowest. In the 208 km away, the 6.69 km/sec layer is downwarping, 6.93 km/sec, 7.17 km/sec layer uplift, and the position is agreed with the bound of Okchon Zone and Kyonggi Massif.

In the profile D-D' (38°N, 126°E~38°N, 129.5°E), there are the 6.65 km/sec layer uplift in 104 km (near Pochon) from the west point of the profile, and anisotropy zones in the upper crust near Kangnung area, 260 km from the west point. We are not sure that this may be related to the fault system that caused historical earthquakes in Fig. 7. We note that in 260 km depart from west starting point, 6.65 km/sec layer is descending, but 6.9 km/sec, 7.14 km/sec layer uplift, from here to east, it is the ocean crust.

In the profile E-E' (38.5°N, 126°E~38.5°N, 129.5 °E), the isovelocities of the upper and the lower crust are downwarping in the 228 km from the west point of the profile, it is the position of continent shelf to ocean, various velocity layers descend then horizontally to east, the depth of Moho in ocean is 28 km. We noted that in the east of 76 km from the west starting point the 6.89 km/sec layer rises.

The profile F-F' is along 36.5 (N, 126°E~38.5°N, 126°E, this profile represents the transfer from the ocean (Yellow Sea) crust to the continental crust. In the 170 km from the south starting point, the isovelocities of the upper and the lower crust uplift,

The sediment is thin the Moho is deeper. Here is the landing from Yellow Sea.

The profile G-G' (36.5°N, 126.5°E~38.5°N, 126.5 °E) has stronger variation of isovelocities in the upper crust. From the south starting point of this profile, 6.40 km/sec, 6.60 km/sec layer rise, and the highest point is near the Seosan, At 50 km from the starting point, i.e. around Inchon, Seoul, the 6.60 km/sec and 6.40 km/sec layers are descending, and the Conrad rises. In 166 km, 6.60 km/sec and 6.40 km/sec layers drop, but 6.57 km/sec and 6.99 km/sec rise with a symmetry at the conter. This may be related to the start of the Chugaryong Rift Zone.

The profile H-H' (36.5°N, 127°E~38.5°C, 127°E) has similar feature with profile G-G', but here it is land We note that within a range of 140 km to the south and north. there are different feature layers of 6.45 and 6.80 km/sec. The corresponding location is near Cholwon, north of Seoul, We note that there is a lower velocity of the lower crust and it is symmetrical body of 6.45 km/sec at the center. The velocity at the center is much lower than that at both ends. In north of Seoul, the velocity increases symmetrically with 6.80 km/sec and 6.99 km/sec of the ridge type in the lower crust, whereas 6.45 km/sec drop with an embedded low velocity layer of 5.91 km/sec in the upper crust, This may be associated with the Chugaryong Rift Zone of the Central Korea.

In the profile I-I' (36.5°N, 127.5°E~38.5°N, 127.5 °E) and J-J' (36.5°N, 128°E~38.5°N, 128°E), various isovelocities layer drop from 55.5 km from the south starting point, in here the Kyonggi Massif transfer to Okchon Zone. We note that there is a fault in the 111 km of profile, and that the isovelocities have stronger downwarping here.

In the profile K-K' (36.5°N, 128.5°E~38.5°N, 128.5 °E), the basement and other isovelocities of the upper crust drop from south starting point to north and the deepest point is in 56.5 km, corresponding to Maepo, here is a boundary of Ryongnam Massif and Okchon Zone. In 126.4 km (near the Odeasan) there is another turning point, the isovelocities have different feature from south, from here to north, it is Kyonggi Massif. We found a low velocity zone near the Youngwol area at a depth of 10 km, indicating that it may be related to the source zone of Youngwol earthquake of December 13, 1996.

CONCLUSIONS AND DISCUSSION

The crust is composed from the upper and the lower parts by the interface Conrad. The average velocity in sedimentary is 5.15 km/sec with the thickness of about 3-4 km in general, but for various regions they are not same. The Kyongsang Basin, Seoul, Packtok-san, Chunchon, Soyang Lake, Namp'o plain have deeper sediment. The average basement velocity is 6.11 km/sec.

In the upper crust, the velocity distribution form obviously fluctuates, and some higher (lower) velocity layers (body) are embedded in normal layers. A remarkable feature of the lower crust is the form of lower crust that appears basically horizontal. The depth from 21.3 km to Moho (29.8 km) is the depth scope of the lower crust. The average velocity on the Conrad layer is 7.10 km/sec, and the average depth of Conrad is 21.3 km.

The average depth and velocity of Moho is 29.8 km and 7.97 km/sec. The form represents deeper in SW and NE and shallower in NW (Namp'o plain, Kaesung, Seoul, Inchon) and SE (Kyongsang Basin). The remarkable crustal velocity differences among Pyongnam Basin, Kyonggi Massif, Okchon Zone, Ryongnam Massif and Kyongsang Basin can be found. The different crustal features of ocean and continent crust are obvious. We also found some deep index of Chugaryong Fault Zone at H-H' of Fig. 4b. We also note that north of Seoul has low velocity structures at depth of 20 km and 10 km near the Chugaryong Rift Zone. It turns out that the north of Seoul is seismologically more active than Seoul. I think we need more data of high quality for the precise high resolution tomography. But we can see large anisotropic bodies near Knagnung on C-C' of Fig. 4a and an embedded low velocity layer near the Hongsung area on A-A' of fig. 4a, implying that these anisotropic zones may be associated with the deep faults system in the upper crust. These facts prove that the larger earthquake distribution on Fig. 6 accords with the deep fault system of earthquake areas. Due to lack of computation data at corners at present, four corners of the inversion scope are unreliable. We have to get the interpretation of geology and geophysics for anomalous velocity distribution in seismic toimography.

ACKNOWLEDGEMENTS

This work is supported by the Korean ministry of Science and Technology and STEPI. This research is also partially supported by the Korean ministry of Education (BSRI-97-5420) and the Korean Research Foundation (1996).

REFERENCES

Aki, K. and Lee, W.H. (1976) Determination of three-dimensional velocity anomalies under a seismic array using first P arrival

from local earthquakes 1. A homogeneous initial model. J. Geophys. Res., v. 81, p. 4381-4399.

Backus, G.E. and Gilbert, F. (1967) Numerical applications of a formalism for geophysical inverse problems. Geophys. J. R. astr. Soc., v. 92, p. 125-142.

Benz, H.M. and Smith, R.B. (1984) Simultaneous inversion for lateral velocity variation and hypocenters in the Yellowstone region using earthquakes and refraction data. J. Geophys.Res., v. 89, p. 1208-1222.

Cho, J.D., Choi, J.H., Lim, M.T. and Park, I.H. (1997) The study on the Bouguer gravity anomaly of the Southern part of Korea. Bull. Seis. Asso. Far. East, (SAFE), v. 3 (2), p. 212-224.

Crosson, R.D. (1976) Crustal structure modeling of earthquake data, 1. Simultaneous least square estimation of hypocenters and velocity parameters. J. Geophys. Res., v. 81, p. 3036-3046.

Hawley, B.W., G. Zandt, and R.B. Smith (1981) Simultaneous inversion for hypocenters and lateral velocity variations: an iterative solution with a layered model. J. Geophys. Res., v. 86, p. 7073-7086.

Kim, O.J. (1987) in Geology of Korea, Kyohak-Sa Publishing, Seoul.

Kim, So Gu and Fuchun Gao.,1995. Korean Earthquake Catalogue, Hanyang University. Anhsan.

Kim, S.J and Kim, S.G. (1983) A study on the crustal structure of south Korea by using seismic waves. J. Korean Inst. Mining Geol., v. 16, p. 51-61.

Kim, S.K and Jung, B.H. (1985) The crustal structure of the southern part of Korea. J. Korean Inst. Mining Geol., v. 18, p. 151-157.

Kim, So Gu and Lee, Seoung Kyu (1994) Crustal modeling for the southern parts of the Korean Peninsula using observational data and ray method. Kor. Inst. Min. and Energy Res., v. 31, p. 549-558.

Kim, So Gu and Qinghe Li (1998) 3-D Crustal Velocity Tomography in the Central Korean peninsula. Shalheveth Freier First International Workshop on advanced Mehod in Seismic Analysis, High Precision Hypocenter Location and Seimic Tomography. Dead Sea, January 12-15, 1998.

Koch, M. (1985a) A theoretical and numerical study on the determination of the 3-D structure of the lithosphere by linear and non-linear inversion of teleseismic traveltimes. Geophys. I.R. astr. Soc., v. 80, p. 73-93.

Koch, M. (1985b) Non-linear inversion of local seismic travel times for the simultaneous determination of 3D velocity structure and hypocenters-application to the seismic zone Vrancea. J. Geophys., v. 56, p. 160-173.

Koch, M. (1993) Simultaneous inversion for 3-D crustal structure and hypocentres including direct, refracted and reflected phase-I. Development validation and optimal regularization of the method., II. Application to the northern Rhine Graben/Rhenish Massif Region, Germany., III. Applicationto the southern Rhine Graben seismic region, Germany. Geophys. J. Int., v. 112, p. 385-447.

Lees, L.M. and Crosson, R.S. (1989) Tomographic inversion for three-dimensional velocity structure at Mount St. Helens using earthquakes data. J. Geophys. Res., v. 94. p. 5716-5728.

Li Qinghe. (1994) The 3-D seismic velocity structure in the northern segment of the North-South Seismic Zone. in Changma earthquake and research of M7 earthquakes. Seismological Press. Beijing.

Li Qinghe., Zhang Yuansheng., Sheng Guoying and Fan Bing (1994) The 3-D seismic velocity structure in Hexi-Corrido, China., in Basic research on the dangeous area in the middle segment of Qilianshan Mountain. Seismological Press, Beijing.

Liu Futian. (1984) Simultaneous inversion of earthquake hypocenters and velocity structure (I)-theory and method. Acta. Geophys. Sini. v. 27, p. 167-175.

Masaitisa, V.N. (1964) Geology of Korea (in Russian). Nedra, Moscow, 264p.

Sambridge, M.S. (1990) Non-linear arrival time inversion: constraining velocity anomalies by seeking smooth models in 3-D. Geophys. J. Int., v. 102, p. 633-667.

Tarantola, A. (1987) Inverse problem theory, methods for data fitting and model parameter estimation. Elsevier, Amsterdam, New York.

Tarantola, A. and Valette, B. (1982) Generalized nonlinear inverse problems solved using the least square criterion. Rev. Geophys. Space Phys., v. 20, p. 219-232.

Thomson, C.I. and Gubbins, D. (1982) Three-dimensional lithospheric modeling at NORSAR: linearity of the method and amplitude variations from anomalies. Geophys. J.R. astr. Soc., v. 71, p. 1-36.

Thurber, C.H. (1983) Earthquake locations and three-dimensional structure in the Coyote Lake area, Central California. J. Geophys. Res., v. 88, p. 8226-8236.

Thurber, C.H. (1985) Nonlinear earthquake location theory and examples. Bull. seismo. Soc. Am., v. 75, p. 779-790.

Walck, M.C. and Clayton, R.W. (1987) P-wave velocity variations in the Coso-region, California, derived from local earthquake travel times. J. Geophys. Res., v. 92, p. 393-405.

Manuscript received 27 March 1998

한반도 중부지역의 3차원 속도 모델 토모그래피 연구

金昭九 · 李清河

요 약 : 직접파, 반사파 및 굴절파를 사용해서 3차원 속도 구조를 결정하기 위한 동시역산 토모그래피 기술을 한반도 중부에 적용하였다. 이곳은 평남 분지, 경기 육괴, 옥천 습곡대, 태백산 습곡대, 영남 육괴, 그리고 경상 분지를 포함한다. 32개 event의 Pg, Sg, PmP, SmS, Pn과 Sn 위상들을 포함한 총 404개 지진파선이 진원 위치와 지각구조 계산을 위해서 역산되었다. 5 (위도 따라 1°)×6 (경도 따라 0.5°)×8 (매 깊이 4 km 두께)의 블럭모델이 역산된다. 따라서 표면에서 Moho까지 8개 단면도, 위도 · 경도를 따라서 8개 측면도, 그리고 Moho깊이 등이 결정된다. 그 결과는 다음과 같다. (1) 퇴적암의 평균속도와 두께는 5.15 km/sec과 3~4 km이다. 기반의 속도는 6.12 km/sec이다. (2) 상부지각에서 속도는 매우 불규칙하나 Conrad 밑의 하부지각의 속도 변화는 근본적으로 변화가 없다. (3) Moho의 평균 깊이와 속도는 29.8 km와 7.97 km/sec이다. (4) 퇴적암 깊이와 속도, 기반암 두께와 속도, 상부지각 Moho 깊이의 모양, 평남 분지, 경기 육괴, 옥천대, 영남 육괴, 경상 분지 등의 현저한 속도 변화가 발견된다. (5) 해양과 대륙 지각의 틀린 지각구조가 분명하다. (6) 추가령 지구대의 저속도 심부 대칭모양이 측면도에서 뚜렷하게 발견되었다. (7) 서울 수도권 지역북부와 홍성지역의 상부지각에서 큰 저속도 이방체가 발견되었는데, 이것은 추가령지구대 및 심부 잠복단층과 관계가 있을 수 있는 큰 속도 이방체로 볼 수 있다.